

1 *Review*

2 **Methods to Grow Better Diffractive Protein Crystals** 3 **Acquired through Space Experiments**

4 **Yoshinobu Hashizume ¹, Koji Inaka ², Naoki Furubayashi ², Masayuki Kamo ², Sachiko
5 Takahashi ¹ and Hiroaki Tanaka ^{2*}**

6 ¹ Confocal Science Inc. 2-12-2 Iwamoto-cho, Chiyoda-ku, Tokyo 101-0023 Tokyo JAPAN;
7 hashizumey@confsci.co.jp (Y.H.), takahashis@confsci.co.jp (S.T.), tanakah@confsci.co.jp (H.T.).

8 ² Maruwa Foods and Biosciences Inc. 170-1 Tsutsui-cho, Yamato-Koriyama, Nara 639-1123 JAPAN;
9 inaka@maruwafoods.jp (K.I.), furubayashi@maruwafoods.jp (N.F.), masayuki_kamo@maruwafoods.jp
10 (M.K.).

11 * Correspondence: tanakah@confsci.co.jp; Tel.: +81-3-3864-6606 (H.T.)

12

13 **Abstract:** We summarize how to obtain protein crystals from which better diffraction images
14 can be obtained. In particular, we describe in detail the quality evaluation of the protein
15 sample, the crystallization methods and crystallization conditions, the flash-cooling
16 protection of the crystal, and crystallization under a microgravity environment.

17 **Keywords:** protein crystallization; protein sample qualification; JAXA PCG; microgravity
18

19 **1. Introduction**

20 We have been providing protein crystallographic services, especially for the Japan Aerospace
21 Exploration Agency's High-Quality Protein Crystal Growth Experiment (JAXA PCG), for many years.
22 Crystallization with a sample from a user often encounters the following issues and challenges: (1)
23 Crystals cannot be obtained with good reproducibility; (2) crystals showing sufficient diffraction are
24 not reproducible; (3) crystals are obtained but do not give any sufficient diffractions; (4) users request
25 larger crystals; and (5) users expect better crystal quality from space experiments. We have overcome
26 many of these issues and accumulated experience based on over 500 samples from various users.
27 Many methods have been reported for obtaining protein crystals from which good diffraction images
28 can be obtained. However, this is a comprehensive process, from sample preparation to obtaining
29 diffraction images. This paper explains our experience, which is useful not only for space experiments
30 but also for crystallization in the laboratory.

31 From our experience, we target more rational technology by referring to the previously reported
32 mechanisms of crystal growth [1-4].

33 It is believed that protein crystals are obtained by reducing the solubility of an aqueous solution
34 of proteins by adding a crystallization agent, which is called a "precipitant". However, the protein
35 molecules in the crystals are not precipitates. Instead, they are arranged in a specific order and are in
36 contact with a solvent through solvent channels. In addition, it seems that the concentration of the
37 precipitant inside the crystal is significantly lower than outside, which balances the chemical
38 potential [1].

39 Between the protein molecules aligned in the crystal, various forces exist, such as hydrogen
40 bonds and ionic and van der Waals interactions. Some of these forces are attractive while others are
41 repulsive [5]. In addition, a macroscopic force called interfacial tension also functions at the crystal
42 interface (Figure 1).

43 In a high-quality crystal, it is important to have good alignment, but to do so, these forces need
44 to be uniform. Defects in the crystal will cause stress and strain, resulting in disordered packing.
45 Because the plasticity of the crystals is not large, once a defect occurs, a mosaic occurs in the crystals

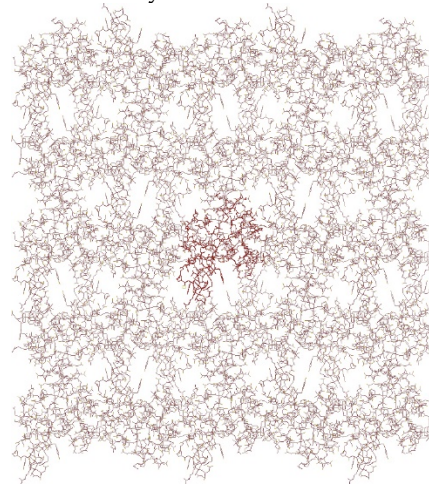
46 [1]. One of the causes of misorientation is homologous impurity [6, 7]. Impurities also greatly reduce
47 the growth rate of crystals [8]. For this reason, it is important that the protein sample used for
48 crystallization is uniform. Therefore, sample preparation is essential to obtaining high-quality
49 crystals from the outset.

50 The second important factor is related to the crystallization conditions. It is important to control
51 the forces between the protein molecules to achieve better alignment by controlling the optimal
52 balance of intermolecular attraction and repulsion, as well as macro interfacial tension.

53 2. Improvement of the sample quality

54 A uniform protein sample is the primary requirement in obtaining high quality crystals that are
55 acceptable for X-ray or Neutron diffraction experiments with certain reproducibility. For this purpose,
56 it is preferable to prepare a sample that is sufficiently stable for a long time. It is also important that
57 samples of equivalent quality are obtained repeatedly. The sample preparation method for this
58 purpose is not covered in this paper. In this paper, the evaluation method of the prepared protein
59 sample and the countermeasures based on the evaluation results are explained.

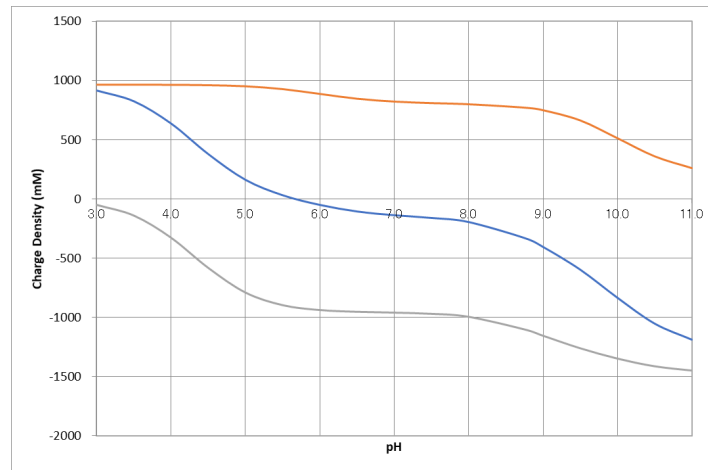
60 It is important to perform accurate evaluations of the protein samples with a relatively easy
61 method. We apply SDS-PAGE, Native-PAGE, two-dimensional electrophoresis, high-resolution ionic
62 exchange, or gel chromatography and Dynamic Light Scattering (DLS) and then comprehensively
63 evaluate the results. From our experience, a sample with high uniformity and consistency with the
64 calculated value of electric charge density [9] empirically has a high possibility of growing crystals of
65 high quality. If the molecules taken in the crystals are different in their molecular weights, or if the
66 electric charge is non-uniform even though the molecules are equal in their molecular weights, a
67 disturbance of the arrangement of molecules in the crystal will be directly produced because
68 molecules close to each other interact due to an electrostatic dipole moment in the crystals. As a result,
69 this phenomenon has serious effects on a crystal's formation and its quality.



70 Figure 1. Protein molecular alignment in a crystal. In the crystal, there is close contact between
71 adjacent molecules. Molecules that are homogeneous with one another can be arranged regularly. The
72 incorporation of non-uniform molecules affects the alignment of molecules around them, making it
73 difficult to obtain a good X-ray diffraction image.

74 2.1. Physical property values of protein molecules

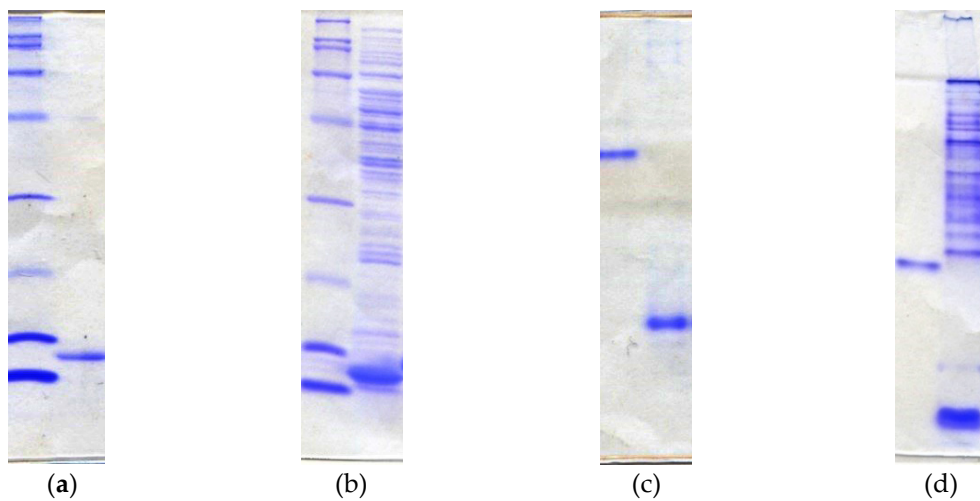
75 Empirically, whether the protein samples can produce high-quality crystals can be evaluated by
76 the deviation between the physical property values of the protein molecules assumed from the amino
77 acid composition and the analysis results described below. Based on the amino acid composition of
78 the protein sample, not only the molecular weight but also the electric charge number at a specific
79 pH can be calculated [10]. Furthermore, the electric charge density can be calculated by dividing this
80 electric charge number by the estimated lattice volume [9] (C-Profile, Confocal Science Inc.) (Figure
81 2).



82 Figure 2. Charge density calculated from amino acid composition. Red line: positive charge density;
 83 gray line: negative charge density; blue line: total charge density.

84 2.2. *SDS-PAGE*

85 Analysis by sodium dodecyl sulfate polyacrylamide gel electrophoresis (SDS-PAGE) is the most
 86 common method to check the purity of protein samples [11, 12]. SDS added to a protein sample binds
 87 to amino acids of the protein molecule and sometimes denatures the protein, thereby producing
 88 negative charges. Then, the protein molecules with SDS are migrated in a polyacrylamide gel by
 89 imposing an electric field. Smaller proteins migrate faster in the gel matrix, so we can separate protein
 90 molecules by their molecular weights. Beta-mercaptoethanol is also applied to reduce disulfide bonds.
 91 It is important to check whether the band clearly migrates to a position corresponding to the
 92 molecular weight calculated from the target protein sequence (Figure 3a). When some minor bands
 93 emerge or when the main band seems doubled (Figure 3b), a heterogeneous component of the
 94 molecular weight exists in the prepared sample. In this case, some of the expressed protein molecules
 95 have likely been modified, so their molecular weights become heterogeneous or the target protein is
 96 partially digested during the expression / purification process.



97 Figure 3. PAGE analysis of typical protein samples. In all gels, the left lanes are for molecular markers.
 98 (a) The homogenous sample migrates as a single band in SDS-PAGE; (b) the sample containing
 99 contaminated protein gives many bands other than the target protein in SDS-PAGE; (c) the sample
 100 migrates with speed proportional to its charge. The sample with electrical homogeneity migrates as a
 101 single band in Native-PAGE; (d) the aggregate sample migrates as a smear and ladder in Native-
 102 PAGE.

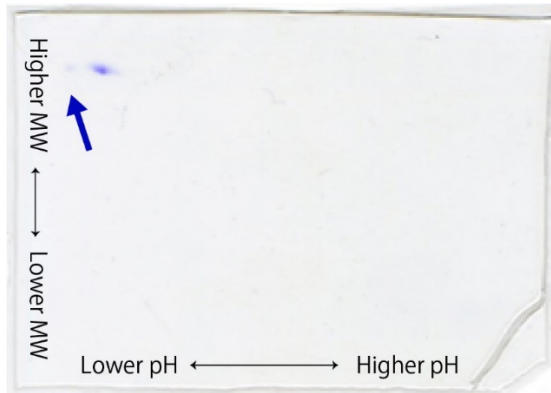
103 2.3. *Analysis by Native-PAGE*

104 The electric charge of a protein molecule varies in accordance with the pH in the solution, and
105 the amount of electric charge can be estimated by calculation. Analyzing with Native-PAGE [11]
106 reveals whether the target protein migrated in accordance with the calculated electric charge (Figure
107 3c, d). The Native-PAGE mentioned here is a simple PAGE analysis in which only SDS is omitted
108 from the solution and the gel. Empirically, it is often observed that even a sample showing a very
109 clear single band in SDS-PAGE gives multiple bands in Native-PAGE.

110 Furthermore, under Native-PAGE, it is often observed that the band migrates to a smear or
111 ladder shape or does not enter the gel. Sometimes, electric charges estimated from the above
112 calculations do not match with the mobility of the band. Perhaps this is caused by some unexpected
113 aggregation of the protein molecules in the solution. Empirically, this phenomenon affects the
114 possibility of crystal formation and crystal quality.

115 *2.4. Two-dimensional electrophoresis*

116 Another method for confirming the uniformity of the electric charge is via two-dimensional
117 electrophoresis [13], which combines isoelectric focusing (IEF) with SDS-PAGE (Figure 4). By using
118 a method where protein samples are separated with IEF prior to SDS-PAGE, the homogeneity of the
119 protein molecule can be shown more clearly. Sometimes, samples with the same molecular weight
120 have slightly different spots (as much as half the pH unit of IEF). These samples often have problems
121 in crystallization.

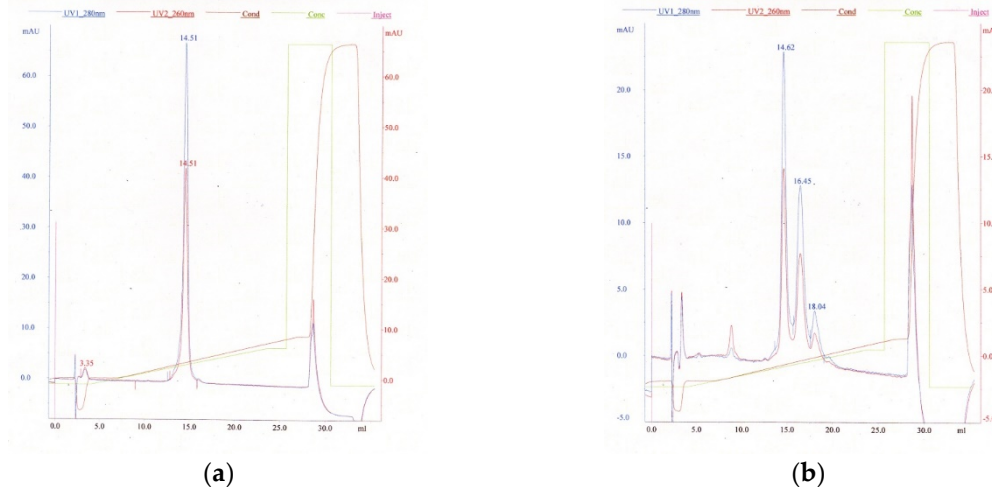


122 Figure 4. A two-dimensional electrophoresis analysis of a protein sample. Horizontal and vertical
123 axes correspond to the pH and molecular weight, respectively. Auto 2D Plus, SHARP LIFE SCIENCE
124 CO is used. With this sample, a crystal with a cluster-like morphology is frequently obtained with
125 about a 1.4 Å resolution. After applying ionic exchange chromatography, a minor component
126 (indicated by the blue arrow) was removed, and a single crystal with a 1.2 Å resolution was obtained.

127 *2.5. High-resolution ion exchange chromatography*

128 High-resolution ion exchange chromatography separates proteins with differences in their
129 surface charges. A Sodium Chloride-gradient for elution from the column is commonly used [14].
130 Samples that can give a sharp and clear peak and elute at an expected concentration of Sodium
131 Chloride (Figure 5a) often give high-quality crystals. On the other hand, proteins that elute as
132 multiple peaks (Figure 5b) contain unexpected problems, and crystallization tends to be difficult.
133 When the heterogeneity of a sample is shown in Native-PAGE and two-dimensional electrophoresis,
134 these samples rarely give one sharp peak on a chromatogram. However, a sharp peak is sometimes
135 observed in chromatography, even when non-uniformity of the electric charge is observed in the
136 results of the Native-PAGE and two-dimensional electrophoresis. It is conceivable that the forming
137 aggregate might not be dissociated during chromatographic separation. This will result in a
138 significant difference between the Sodium Chloride concentration (where the peak is eluted) and the
139 calculated charge density of the target protein. There are various kinds of ion exchange resins with

140 different chromatographic particles (e.g., a quaternary ammonium group and a carboxymethyl group)
141 [15].



142 Figure 5. Typical chromatogram of Ion-exchange chromatography. Blue and red lines show UV
 143 absorption at 280 and 260 nm, respectively. Brown and green lines show the actual and programmed
 144 Sodium Chloride concentration: (a) a homogeneous sample of a protein that gives a high-resolution
 145 single crystal beyond 1.1 Å; (b) a heterogeneous sample of the same protein that gives a poor crystal
 146 with a 1.5 Å resolution.

147 2.6 High-resolution gel chromatography

High-resolution gel chromatography separates proteins with differences in their molecular weights and can be applied to all proteins, from those with high to those with low molecular weights. Various gels have been developed for each molecular weight. Protein molecules often form a dimer, tetramer, or n-mer in a solution and can be detected by high resolution gel chromatography. This technique can also detect much larger aggregates. Even with a relatively low-molecular-weight protein molecule, some molecules may associate nonspecifically in a solution to form a high-molecular-weight aggregate. The presence of such an aggregate often hinders crystallization. Gel chromatography can effectively remove such aggregates, and high-quality crystals can be obtained.

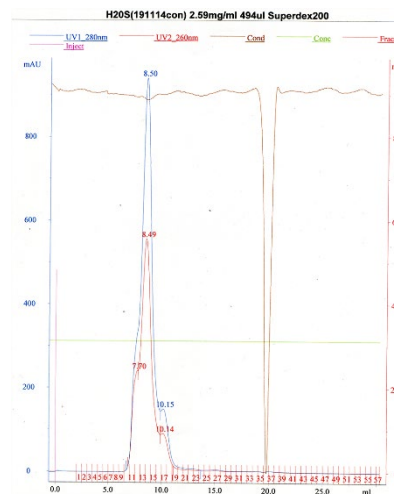
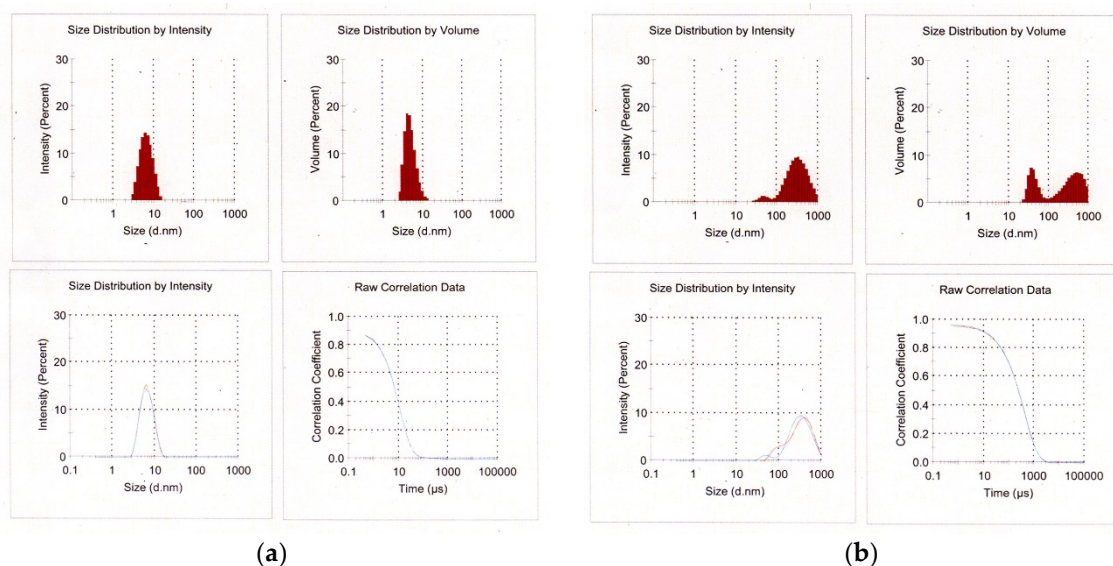


Figure 6. Typical chromatogram of gel chromatography. Blue and red lines show the UV absorption of 280 and 260nm, respectively. The leading and trailing shoulders of the main peak suggest the existence of some different molecular weight components. After removing these components, crystal quality was improved.

161 2.7 Dynamic light scattering method

162 With dynamic light scattering (DLS) measurement, it is possible to determine what the
 163 molecular size distribution is like in the solution. The points to be confirmed from the obtained results
 164 are whether the estimated molecular weight is equal to the integral multiple of its own molecular
 165 weight with a narrow distribution and if there are no large sized particles (mono-modal distribution)
 166 [16]. In many cases, samples with a narrower distribution width of their radii will give high-quality
 167 crystals (Figure 7a). X-ray crystallographic analysis shows that the maximal size of a protein molecule
 168 of about 50 kDa (450 aa) is 4 to 5 nm. If, in the analysis of the DLS measurement, a particle larger than
 169 50 nm emerges, the possibility that this protein molecule will form irregular aggregates must be
 170 considered. From our experience, it is difficult to obtain crystals from such a sample (Figure 7b).



171 Figure 7. Typical results of dynamic light scattering (DLS) calculated by an autocorrelation function:
 172 (a) An appropriate sample of a protein shows narrow and mono-modal distribution; (b) a
 173 heterogeneous sample of the same protein shows a broad and poly-modal distribution.

174 2.8. Measures to improve protein samples

175 2.8.1. Uniformity improvement

176 When multiple bands or spots are found on Native-PAGE, two-dimensional electrophoresis, and
 177 high-resolution chromatography, it is often possible to separate them with high-resolution
 178 chromatography. When peak shoulders or asymmetrical peaks become visible, such as leading or
 179 tailing peaks, those peaks may be separated by reconsidering the elution condition (chromatography
 180 particle, resins, buffers, and gradient programs) to provide high-resolution separation.

181 In this case, the components to be separated are as follows:

- 182 ➤ Other proteins, lipids, etc., which failed to be removed through other purification steps;
- 183 ➤ Proteins whose N or C terminal ends are not processed correctly;
- 184 ➤ Proteins including irregularly modified residues.

185 Sometimes, when these contaminants are removed, the total amount of target protein is reduced,
 186 so it is necessary to design an expression host and expression plasmid carefully to avoid unexpected
 187 processing or modification.

188 2.8.2. Aggregate removal

189 It is difficult to overcome irregular aggregates in the sample, and it is necessary to determine
 190 what caused such irregular aggregates through the purification process. From our knowledge, the
 191 probable causes are as follows:

192 ➤ Denatured proteins caused by the concentration process in the crude state or ammonium
193 sulfate precipitation. Avoiding these processes might improve the sample.
194 ➤ Aggregated proteins associated with contaminants or isozymes with different isoelectric
195 points (pIs) through hydrophobic or hydrophilic interactions. Dialysis, gel filtration, or
196 high-resolution chromatography sometimes remove such aggregates, which might
197 dramatically improve the sample quality.

198 *2.8.3. Improvement of sample quality deterioration over time*

199 It is often observed that samples for crystallization undergo degradation. Quality changes,
200 associated with time (sample degradation and increase of aggregates), can be evaluated by the
201 methods mentioned above. From our experience, effective countermeasures are as follows:

202 ➤ For unstable proteins, it is advised to construct mutants to improve their stability [17].
203 ➤ In the case of protease degradation, adding protease inhibitors followed by removing
204 proteases in the subsequent chromatography step is usually effective.
205 ➤ In the case of damage caused by oxidation, it is advised to purify, store, and crystallize the
206 samples under a deoxygenated state.

207 **3. Crystallization**

208 *3.1. Reagent*

209 It is well known that proteins can be crystallized by mixing protein samples and crystallization
210 reagents. Generally, protein solubility is decreased by this operation [1, 2, 4]. A component in the
211 crystallization reagent that dramatically reduces the solubility of the protein is called a precipitant.
212 However, a “precipitant” is not expected to produce a true protein precipitate but to separate protein
213 molecules in a specifically ordered phase inside a crystal, the outside of which is in a freely dispersed
214 phase. Frequently used precipitants are as follows [18]:

215 ➤ Salts—a combination of mono- or multi-valent anions and cations, for example, Ammonium
216 Sulfate, Sodium Malonate, etc. The tendency for lowering solubility is listed in the
217 Hofmeister Series [19]. In general, anions and cations have various effects other than simply
218 reducing solubility. Therefore, determining a proper salt for crystallization is accompanied
219 by some difficulties.

220 ➤ Polymers—high-molecular-weight polymers, for example, polyethylene glycol (PEG). The
221 mechanism for reducing solubility is explained as an excluding volume effect [1]. In general,
222 the preferable molecular weight of PEG is related to the target protein [20], although a
223 molecular weight of 400 to 20,000 is frequently used. Lower-molecular-weight PEG, such as
224 PEG 400, has the ability to denature some proteins, which is similar to the effects of an
225 alcohol. However, a higher-molecular-weight PEG does not have significant side-effects
226 other than reducing solubility. Thus, high-molecular-weight PEG is easier for controlling the
227 crystallization process and is frequently used in crystallization.

228 ➤ Organic solvents and alcohols—for example, 2-methyl-2,4-pentanediol (MPD), isopropanol,
229 etc. This mechanism is explained as reducing the dielectric constant of the solution [1]. Some
230 hydrophobic proteins sometimes prefer organic solvents.

231 In general, these precipitants are used in significantly higher concentration, such as several tens of
232 weight per volume percentage.

233
234 In addition to these main precipitants, some amounts of additives are frequently used. These
235 additives are summarized in Table 1. In the case of a crystallization solution consisting of a large
236 number of components, it is quite difficult to accurately estimate each component's effects on
237 crystallization, even though there may be some synergistic effects [18]. However, by understanding

238 the protein concentration and phase diagrams of these components as coordinate axes, it is possible
 239 to grasp their effects on crystallization, which is useful for a more rational optimization of
 240 crystallization conditions. In the batch method, the fixed crystallization condition is one point on the
 241 phase diagram and is not changed, which is suitable for this investigation. In other methods, the
 242 condition varies with time on the phase diagram, which induces some complicated phenomena. Thus,
 243 it is necessary to understand the differences between each method.

244 Table 1. Frequently used additives in crystallization solutions.

Effect	Classification	Reagent and usage example	Explanation
Electrostatic interaction	Counter ion	10–1000 mM Sodium Chloride	Reduces the electrostatic repulsion between protein molecules by creating an ion pair on the protein molecule surface [19]. Na^+ and Cl^- are the most conventional ones.
	Organic solvent	5%–20% MPD 5%–20% Dioxane	Reduces the electrostatic repulsion between protein molecules by reducing the dielectric constant of the solvent [1].
Specific intermolecular interactions	Multivalent acid	10–200 mM Tartrate	Intervenes and attracts between protein molecules
	Multivalent metal ion	10–200 mM MgCl_2	
	Multivalent base	10–200 mM Bis Tris Propane	
pH buffering	Weak acid	10–100 mM Acetate	Buffer pH of solution
	Weak base	10–100 mM Tris	
Solubilizing	Detergent	0.1%–2% DDM (n-Dodecyl-beta-D-maltopyranoside)	Solubilization of protein with strong hydrophobicity of the membrane protein [21, 22]

245 A few heuristics are as follows:

- 246 ➤ In the case of PEG, as the concentration increases, the number of generated crystals
 247 increases once but decreases as the concentration of PEG further increases. It is thought that
 248 the nucleus formation probability decreases as the viscosity increases [23, 24, 25]. Further,
 249 in a state where the nucleation formation probability is lowered, the degree of
 250 supersaturation is high, so secondary nucleation on the crystal surface is likely to occur,
 251 and cluster crystals are likely to be formed.
- 252 ➤ When there is no reagent that enhances intermolecular interactions, a reduction of
 253 electrostatic repulsion is necessary for crystallization. Neutralization by Na^+ and Cl^- as
 254 counterions of the divergent groups ($-\text{COO}^-$, $-\text{NH}_3^+$) of proteins is one of these methods. In
 255 this case, it is advisable to add Sodium Chloride at a concentration in relation to the electric
 256 charge density [9, 19].
- 257 ➤ Ions such as Na^+ and Cl^- not only interact with dissociation groups on the protein surface
 258 but also interact with other acids and bases and affect their effects. Therefore, when these
 259 ions coexist with a reagent that enhances intermolecular interactions, conversely, the effect
 260 is diminished.

261 3.2. Crystallization method

262 Methods of protein crystallization have been developed to allow a large number of conditions
 263 to be studied with a small number of samples. Typical crystallization methods are as follows.

264 3.2.1. *Batch method*

265 The batch method is the oldest and simplest method for protein crystallization [26]. In the batch
266 method, a protein sample and a crystallization reagent solution (reservoir solution) are mixed at an
267 appropriate ratio and left to stand. As long as crystallization does not start, the concentration of the
268 components in the solution does not change. Therefore, this is a good method to study crystallization
269 after fixing the concentration of each reagent in the solution precisely [Figure 8a].

270 3.2.2. *Vapor-diffusion method*

271 In the vapor-diffusion (VD) method [27, 28], a solution prepared by mixing a protein sample and
272 a crystallization reagent solution (reservoir solution) in a ratio of typically 1:1 interacts with a
273 reservoir solution via an air layer.

274 By 1:1 mixing, the concentration of other components coexisting with the protein sample, the
275 concentration of the protein sample and the crystallization reagent derived from the reservoir, and
276 the coexisting components initially become halved, but water migrates due to its interactions with
277 the reservoir and concentrates [27, 28]. As a result, all the concentrations increase toward the original
278 level, and crystallization occurs when the concentrations allow crystals to be formed in the process.
279 In many cases, it is more likely that crystals are grown if all the concentrations, including proteins,
280 increase at the same time. Therefore, crystals are easier to grow by the VD method. On the other hand,
281 with this method, it is not possible to control these concentrations individually. For this reason, there
282 are cases where crystals cannot be obtained—for example, when other components coexisting in the
283 protein sample are not favorable for crystallization.

284 The VD method is the most commonly used method for many researchers. A large number of
285 screening kits for searching for crystallization conditions are also on the market, but all components
286 are concentrated in this method (Figure 8b).

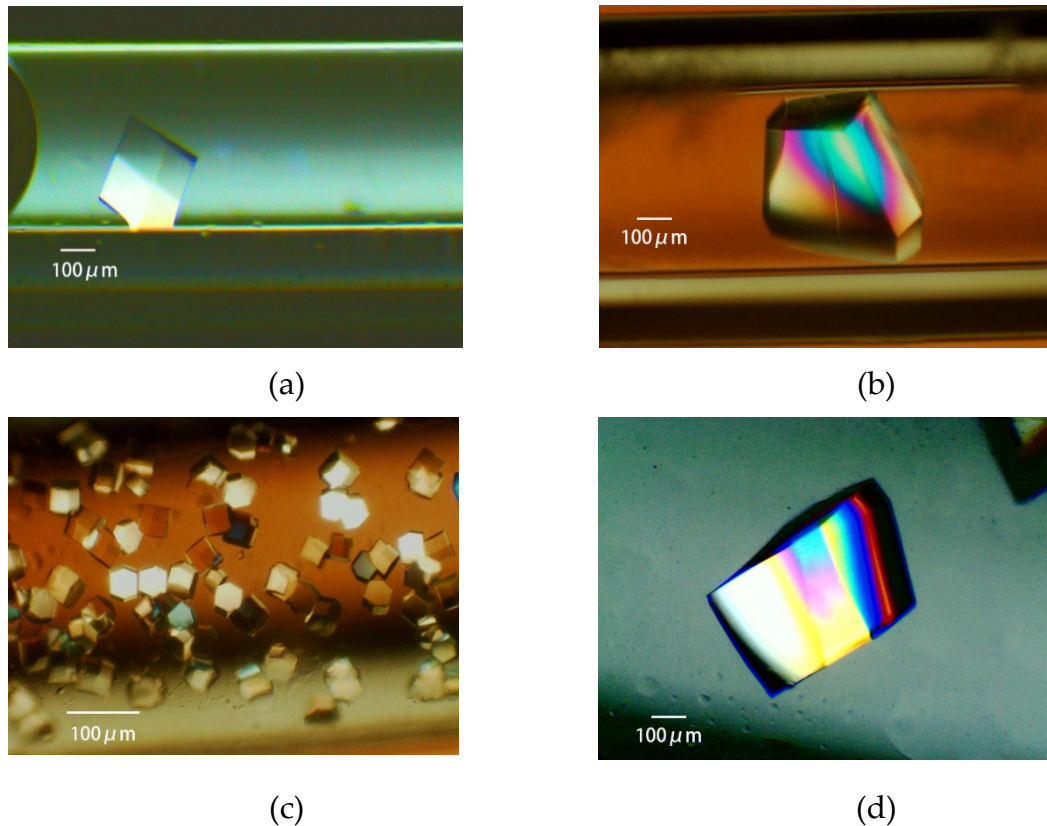
287 3.2.3 *Counter-diffusion method*

288 The counter-diffusion (CD) method [29, 30] generally fills a capillary with a protein sample and
289 diffuses the crystallization reagent components from the capillary end. At the same time, the protein
290 sample in the capillary and other coexisting components diffuse outside the capillary. Therefore, the
291 coexisting components in the capillary are replaced by the components in the reservoir solution. As
292 a result of this bidirectional diffusion, a combination of the wide concentration regions of the
293 crystallization reagent and the protein sample is scanned.

294 The Granada Crystallization Box (GCB) places an agarose gel layer between a protein solution
295 and a crystallization reagent to achieve relatively mild solution diffusion. This method enables
296 screening of infinite crystallization conditions in one capillary [31]. We modified this method and
297 used a gel-tube instead of the agarose gel layer to simplify this method [32].

298 The time course of bidirectional diffusion is not easy to measure. Therefore, we prepared a one-
299 dimensional (1-D) diffusion simulation program so that various concentration components in the
300 capillary can be estimated [32]. It is necessary to consider the correlation between this diffusion time
301 course and the crystallization start time on the phase diagram when studying crystallization
302 conditions.

303 The component with the smaller molecular weight diffuses quickly, and the component with the
304 larger molecular weight, such as the protein, slowly diffuses. Therefore, among the other components
305 coexisting with the protein molecules inside the capillary, a component having a low molecular
306 weight diffuses faster and leaks out of the capillary. On the other hand, the main crystallization
307 reagent component of the reservoir and the coexisting components diffuse into the capillary.



308 Figure 8. The lysozyme is crystallized with four crystallization methods [36]. (a): Batch method. A
309 solution of 18 mg/ml protein, 15% polyethylene glycol (PEG) 4000, 400 mM Sodium Chloride, and 50
310 mM Sodium Acetate Buffer pH 4.5 is loaded in a 0.5 mm bore capillary. (b): Vapor diffusion method.
311 20 mg/ml protein in 50 mM Sodium Acetate Buffer pH 4.5 is mixed with an equal volume of reservoir
312 solution containing 10% PEG 4000, 600 mM Sodium Chloride, and 50 mM Sodium Acetate Buffer pH
313 4.5. The mixture was loaded in a 0.5 mm bore capillary, and interacted with the reservoir solution, as
314 shown in [36]. (c): Counter diffusion method. A solution of 25 mg/ml protein, 20% PEG 4000, and 50
315 mM Sodium Acetate Buffer pH 4.5 is loaded in a 1 mm bore capillary. After the Gel-Tube is plugged
316 [36], the capillary is placed in a reservoir solution containing 20% PEG 4000, 1000 mM Sodium
317 Chloride, and 50 mM Sodium Acetate Buffer pH 3.5. (d): Dialysis method. A solution of 25 mg/ml
318 protein, 5% PEG 4000, and 50 mM Sodium Acetate Buffer pH 4.5 is loaded in a 2 mm bore capillary
319 with a dialysis membrane [36]. The capillary is placed in a reservoir solution containing 10% PEG
320 4000, 700 mM Sodium Chloride, and 50 mM Sodium Acetate Buffer pH 4.5.

321 In the CD method, the volume of the reservoir is usually much larger than the capillary content,
322 so components other than the protein molecules in the capillary are replaced with reservoir
323 components. Therefore, the concentrations of the reagent components related to the crystallization
324 conditions can be individually controlled, and more advanced crystallization conditions can be set.
325 For example, in cases where the crystals are not obtained by the VD method, such as when some of
326 the components coexisting in a protein sample are not favorable for crystallization, high-quality
327 crystals have often been obtained by the CD method.

328 The diffusion of protein molecules is greatly reduced in PEG, whereas the diffusion of low-
329 molecular-weight compounds does not slow-down in PEG [33]. Therefore, when a PEG-type
330 crystallization reagent is applied to the CD method, the diffusion leakage of proteins from the
331 capillary can be suppressed, which is preferable. There are not many studies that use the CD method.
332 However, having a good understanding of the mechanism as described above when setting
333 crystallization conditions is a good way to obtain crystals with more optimal crystallization
334 conditions than other methods (Figure 8c).

335 3.2.4 Dialysis method

336 The dialysis (DL) method replaces the coexistence of components with the protein sample into
337 the reservoir solution while suppressing diffusion leakage of the protein molecules via the dialysis
338 membrane [34, 35]. Therefore, the concentration of the reagent components, related to the
339 crystallization conditions, can be individually controlled; like the CD method, more advanced
340 crystallization conditions can be set. In the general DL method, the Button method has been used. In
341 this method, since the reservoir solution diffuses into the container immediately, problems like the
342 generation of bubbles accompanying a sudden change in osmotic pressure are likely to occur.
343 Recently, we developed a dialysis method with a diffusion path with a dialysis membrane attached
344 to the opening end of the CD method capillary, thereby achieving dialysis under mild conditions [36].
345 A crystal obtained by the DL method in a capillary is shown in Figure 9(c)(d). Few studies use the DL
346 method. However, having a better understanding of the mechanism above when setting conditions,
347 as in the CD method, is a good way to set more optimal crystallization conditions.

348 3.3. Improvement of crystal quality

349 3.3.1. Reproducibility of crystallization

350 When a good-quality protein sample does not reliably reproduce crystals, special care should be
351 taken to maintain the same salts, buffer, and pH as the procedure originally used to crystallize the
352 sample. In general, it is thought that crystallization occurs due to a main crystallization reagent, but
353 other coexisting components greatly influence it. Particularly in the VD method, it should be noted
354 that the components contained in the protein sample are concentrated, like the reservoir components
355 during crystallization.

356 3.3.2. Understanding nucleation rate

357 To control the size and number of crystals, it is preferable to understand the theory behind the
358 nucleation process. Generally, the three-dimensional nucleation rate in crystallization is expressed
359 by the following equation [23, 24]:

$$360 I = \frac{const}{\eta} \times C \times \exp\left(-\frac{16\pi\gamma^3}{3kT(\Delta\mu)^2}\right) \dots\dots\dots (1)$$

361 where η is viscosity, C is the solution concentration, γ is the surface tension, and $\Delta\mu$ is the chemical
362 potential difference between the crystal and the solution of a unit volume.

363 As can be seen from this equation, the rate of three-dimensional nucleation becomes higher as
364 the protein concentration (C) becomes higher, lower when the viscosity (η) is higher, and lower when
365 the interfacial tension (γ) is higher. When the solubility is low, $\Delta\mu$ becomes high, and the nucleation
366 probability increases. When the protein concentration (C) is high, the number of crystals tends to
367 increase. As the concentration of the main crystallization reagent increases, $\Delta\mu$ becomes larger as the
368 solubility decreases, and the number of crystals increases once. However, as the
369 interfacial tension (γ) increases further, the number of crystals tends to decrease. With a highly
370 viscous crystallization reagent like PEG, when the viscosity (η) further increases, the crystal number
371 significantly decreases. For a crystallization method in which the concentration of the main
372 crystallization reagent increases with the passage of time, it is better to be conscious of how the three-
373 dimensional nucleation rate has passed. Not only the main crystallization reagent but also the
374 counterion, multivalent cation, and polyvalent anion may possibly lower solubility. One must choose
375 the reagents to be added by considering how much of a plus or minus electric charge the protein has
376 at the pH needed for crystallization.

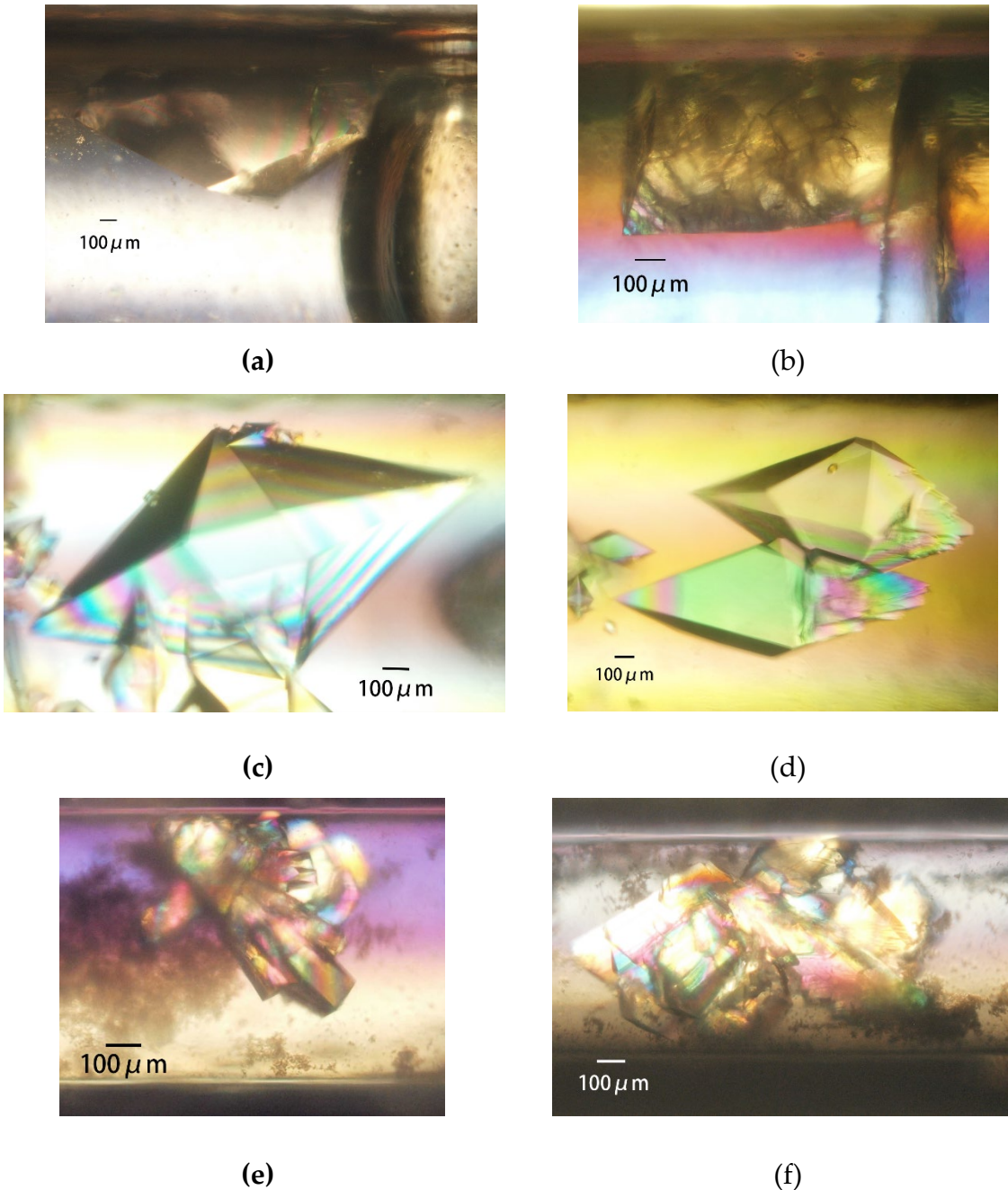


Figure 9. Space and ground grown crystals. PCCel6A crystals grown in space (a) and terrestrially (b) by the counter-diffusion (CD) method; 39.3 mg/ml PCCel6A, 90 mM Sodium Chloride, 10 mM Cellotriose in 5 mM Tris-HCl pH7.5 is loaded in a 2 mm bore capillary. After the Gel-Tube is plugged [36], the capillary is placed in a reservoir solution containing 46.4% PEG 4000, 5 mM Cellotriose, and 50 mM Sodium Acetate pH 4.5. Thaumatin crystals grown in space (c) and terrestrially (d) by the dialysis (DL) method; 33.7 mg/ml Thaumatin in 50 mM HEPES pH 7.0 is loaded in a 2 mm bore capillary with a dialysis membrane [36]. The capillary is placed in a reservoir solution containing 25% PEG 4000, 100 mM Sodium Chloride, 75 mM Sodium Tartrate, and 50 mM HEPES pH 7.0. H-Protein crystals grown in space (e) and terrestrially (f) by the CD method; 38.2 mg/ml H-protein, 25 mM Sodium Chloride, 500 mM Ammonium Sulfite, 20 mM Sodium Citrate pH 3.0, 0.4 mM DTT, and 4% glycerol is loaded in a 0.7 mm bore capillary. After the Gel-Tube is plugged [36], the capillary is placed in a reservoir solution containing 2.5 M Ammonium Sulfate, 25 mM Sodium Chloride, and 100 mM Sodium Citrate pH 3.0.

377 3.3.3. *Obtaining appropriately shaped crystals for diffraction experiment*

378 When a crystal can be obtained, but that crystal becomes needle-shaped or thin plate-shaped
379 and is not suitable for X-ray diffraction experiments, there are usually some problems with the
380 homogeneity of the protein sample. In many cases, it is better to improve the sample quality to
381 overcome these problems. However, there are cases where protein samples are not problematic, yet
382 an appropriate shape is not obtained. In such cases, adding reagents that affect the anisotropic forces
383 between molecules is effective (that is, electrostatic interactions, hydrophobic interactions, and
384 specific intermolecular interactions). It is also possible to change the crystal's shape by changing the
385 pH to the side opposite to the pI and changing the polarity of the electrostatic repulsion.

386 3.3.4. *Avoiding crystal clustering*

387 In a cluster crystal, very fine crystals are gathered, or a single crystal of a certain size seems to
388 grow from the surface of another single crystal. In the former case, there are usually problems with
389 the protein samples, and the first thing to do is to improve the sample quality. In the latter case,
390 although the degree of supersaturation is high, the probability of three-dimensional nucleation is low,
391 such that two-dimensional nuclear growth occurs from the crystal's surface (as the nucleus). In this
392 case, the problem may also be caused by heterogeneous components contaminating the protein
393 sample and can be solved by improving the protein sample. However, this may happen even if the
394 sample has no problem, in which case reducing the supersaturation degree by lowering the protein
395 concentration or lowering the interfacial tension or viscosity by decreasing the concentration of the
396 main crystallization reagent are effective.

397 3.3.5. *Resolution and Molecular packing problem*

398 Although crystals are obtained, the resolution of the X-ray diffraction may not be high enough
399 to obtain the expected accuracy during structural analysis. Moreover, there may be numerous
400 molecules in the asymmetric unit, so structural analysis may be difficult. If the uniformity of the
401 protein sample is insufficient, an improvement of the sample quality is necessary first. When the
402 sample has no problems, these problems may be solved by a number of different means, including
403 changing the force between the molecule to change the packing. Some of the means that have
404 achieved success are as follows:

- 405 ➤ Increasing the concentration of the main crystallization reagent: The interfacial tension
406 increases, and a bulk force from the crystal's surface is applied between the protein
407 molecules isotropically, bringing them closer together. As a result, the interaction between
408 the neighboring protein molecules increases, the disorder is reduced, and the resolution
409 increases.
- 410 ➤ Reducing the counter ions: The electrostatic repulsion force increases, which is the micro
411 anisotropic force between the molecules. As a result, a protein's molecular alignment is
412 more sensitive to its surface charge distribution, and the molecules are aligned in a more
413 uniform direction.
- 414 ➤ Adding metal ions, organic acids, and organic bases: Some of these have an attractive
415 function between protein molecules to align the molecules with micro anisotropic forces
416 between them.
- 417 ➤ Changing the pH of the crystallization condition to the opposite side of the protein's pI:
418 This changes the polarity of the electrostatic repulsive force acting between the protein
419 molecules and changes the micro anisotropic force acting between them, so the packing
420 may change greatly.

421 3.4. *Growing large crystals*

422 Today, a crystal of 1 mm³ or more is necessary for neutron diffraction experiments [37].
423 Compared to crystals for general X-ray diffraction experiments (i.e., ~5 μm, taken on microfocus X-

424 ray beamlines), this value is 100 times or larger, which represents a bottleneck for neutron diffraction
425 experiments.

426 In order to obtain large crystals, it is necessary to find a condition under which the number of
427 crystals produced per unit volume is approximately one and to grow the crystal while controlling the
428 appropriate crystallization conditions. These include experimental strategies utilizing solubility
429 diagrams, ripening effects, classical crystallization techniques, microgravity, and theoretical
430 considerations [37].

431 Nakamura et al. have succeeded in obtaining large crystals by determining such crystallization
432 conditions using phase diagrams and shifting to appropriate crystallization conditions [38]. Niimura
433 and colleagues have devised a device capable of reversibly dissolving crystals once produced and
434 have successfully obtained large crystals by reducing the number of crystals [39].

435 The authors succeeded in producing lysozyme crystals with a long side of about 1 mm using the
436 DL method in a capillary, in which a dialysis membrane was attached to a gel tube [40]. The
437 crystallization conditions were optimized by using a three-dimensional phase diagram, in which the
438 main crystallization reagent (PEG) concentration and the counter ion (Sodium Chloride)
439 concentration were changed [25].

440 4. Harvesting crystal and cryo-protection

441 When removing crystals from the crystallization vessel, we often experience crystal damage. For
442 X-ray diffraction experiments with synchrotron radiation, it is necessary to cryoprotect crystals so
443 that there is no damage to the crystal when flash-cooled.

444 4.1. Optimization of the harvest solution

445 In the batch method, since there is no concentration change of the solution component with time,
446 it is often preferable to harvest crystals in the same solution as the batch solution. Using the VD
447 method and the DL (with Button) method, the time to reach equilibrium is short, and its composition
448 approaches that of the reservoir solution, so the reservoir solution can be used for the harvest solution.
449 On the other hand, in the CD method and DL method with a diffusion path, it takes time to diffuse
450 the crystallization reagent inside the capillary. This tendency is particularly remarkable when a high-
451 molecular-weight PEG is used as a reagent. Even after two to three months have elapsed since filling
452 in the capillary, the concentration of the crystallization reagent inside the capillary is not in
453 equilibrium, and its concentration varies depending on the location in the capillary. Due to the
454 difference in the reagent concentration at the location where the crystals were grown, if the wrong
455 harvest solution is used, the crystals are destroyed or damaged due to osmotic shock, and the quality
456 of the crystals is markedly degraded.

457 In order to avoid this phenomenon, the time change of the reagent concentration at each point
458 inside the capillary is calculated in advance with a 1-D simulation program [32]. Based on the place
459 where the crystal was actually obtained and the elapsed time after the setup, the crystallization
460 reagent concentration can be estimated for the preparation of the harvest solution.

461 4.2. Treatment of crystals obtained in a capillary

462 In the batch method, the VD method, and the DL (with Button) method, crystals can be taken
463 out directly from a crystallization drop with a cryo-loop. On the other hand, when crystals are
464 generated in a capillary, such as in the CD method and DL (with a diffusion path) method, it is
465 necessary to carry out considerably detailed work using a stereoscopic microscope in order to remove
466 the crystals intact. It is necessary to observe, in detail, the capillary where the crystals are formed and
467 decide which crystal is best for extraction. The capillary is cut with a range of about 5 mm in front of
468 and in the back of the crystal. The cut capillary segment that contains the targeted crystal is held by
469 tweezers, and the harvest solution is poured into one side of the capillary with a micropipette. If all
470 goes well, the crystals will remove themselves from the capillary wall and become pushed out to be
471 gathered with a cryo-loop.

472 If crystals continue to adhere to the inner wall of the capillary and do not come out even after
473 applying the harvest solution, a thin wire is used to grind the crystal and remove it from the capillary
474 wall.

475 *4.3. Cryo-treatment of crystals*

476 During a diffraction experiment using synchrotron radiation, crystals should usually be flash-
477 cooled for protection from radiation damage. When flash-cooling crystals, it is necessary that the
478 solution around the crystal be solidified into a glassy state [41]. For this reason, crystals are passed
479 through a cryoprotectant solution prepared by adding cryoprotectant to the harvest solution, and the
480 solution around the crystal is replaced. Empirically,

481 ➤ Ensure that the drops of cryoprotectant solution can be flash-cooled into a glassy form in
482 advance.

483 ➤ In the case of PEG alone as a cryoprotectant, a concentration of about 35% or more is
484 desirable.

485 ➤ In the case of a PEG type of a lower concentration in the harvest solution, it is preferable
486 that PEG or glycerol is added to a total concentration of about 35% or more. However, as
487 the amount of glycerol to be added increases, the osmotic pressure difference becomes large,
488 so one must be careful with this process.

489 ➤ In the case of salt in the harvest solution, when glycerol cannot be added, sucrose or
490 trehalose is the next choice.

491 **5. Optimization for microgravity conditions**

492 *5.1. Introduction*

493 In the crystallization of proteins in space experiments, the problems of crystallization may be
494 alleviated by the effects of microgravity [1, 42-45]. Crystal clustering and disordering are suppressed,
495 and the resolution of X-ray diffraction is improved [46]. Some examples of space and ground-grown
496 crystals are shown in Figure 9. Moreover, although the reason is unknown, nucleation formation is
497 suppressed, crystals are increased in size, and, in some cases, crystals with different space groups are
498 grown.

499 In the solution around the growing crystal, protein molecules are incorporated into the crystal
500 surface, and the density of the solution is lowered [1, 47, 48]. In the terrestrial environment, a density-
501 driven flow occurs. As a result, protein molecules are continuously transported by this flow from a
502 place far away from the crystal into the solution. Impurities and minute crystals in the solution are
503 also carried and taken into the surface of the crystal. On the other hand, in a microgravity
504 environment, protein molecules, impurities, and minute crystals approach the crystal's surface only
505 by thermal motion. As a result, their concentration on the crystal's surface decreases compared to
506 that under a terrestrial environment.

507 Indeed, Otálora et al. [47] confirmed by optical interferometry that a protein depletion zone
508 (PDZ) was formed in the vicinity of growing lysozyme crystals in space experiments (STS-95) during
509 the 1998 Space Shuttle mission. It is believed that if the protein concentration on the growing crystal's
510 surface decreases due to the formation of PDZ, the supersaturation degree decreases, the growth rate
511 decreases, and the disorder of the protein molecule taken in the crystal decreases. Thomas et al. [48]
512 also revealed that impurity uptake is greatly suppressed in lysozyme crystals grown in a
513 microgravity environment in the space experiment (STS-95). It is thought that this is due to the
514 formation of an impurity depletion zone (IDZ) around the crystal, which decreases impurity
515 incorporation in the crystal. For the same reason, if the adhesion of minute crystals decreases, not
516 only disordered reduction but also the suppression of clusters may be expected. On the other hand,
517 according to Vekilov et al. [49], fluctuation occurs in the crystal growth rate due to the interaction
518 between density-driven convection and the molecular uptake process into the crystal, and, as a result,
519 this fluctuation conceivably causes disorder by step bunching. Therefore, the suppression of density-

520 driven convection also solves this problem. Incidentally, a method and apparatus for growing
 521 crystals with less disorder (even in a terrestrial laboratory) has been devised by suppressing the
 522 degree of supersaturation or, conversely, imparting flow actively to the crystal's surface, which may
 523 suppress step bunching [50].

524 *5.2. Space experiment model*

525 For the diffusion field formed around the growing crystal, a numerical analysis can be
 526 performed with a simplified model system, assuming that the crystal is a sphere and ignoring the
 527 dissociation of protein molecules and impurity molecules from the crystal. The effect of formation of
 528 PDZ is defined as the DFR (Driving Force Ratio), and the effect of suppressing the impurity uptake
 529 via the formation of IDZ is the IR (Impurity Ratio) [51-53]:

$$530 DFR = \frac{DF_{0G}}{DF_{1G}} = \frac{C(R) - Ce}{C(\infty) - Ce} = \frac{\frac{R \cdot \beta \cdot Ce}{D} + C(\infty)}{1 + \frac{R \cdot \beta}{D}} - Ce = \frac{1}{1 + \frac{R \cdot \beta}{D}} \dots\dots(1)$$

$$531 IR = \frac{IUR_{0G}}{IUR_{1G}} = \frac{\frac{\beta i Ci(R)}{\beta(C(R) - Ce)}}{\frac{\beta i Ci(\infty)}{\beta(C(\infty) - Ce)}} = \frac{\frac{\beta i (1 + \frac{R \beta}{D})}{\beta (1 + \frac{R \beta i}{D})} \frac{Ci(\infty)}{C(\infty) - Ce}}{\frac{\beta i Ci(\infty)}{\beta(C(\infty) - Ce)}} = \frac{1 + \frac{R \beta}{D}}{1 + \frac{R \beta i}{D}} \dots\dots(2)$$

532 where DF_{0G} and DF_{1G} are the microgravity and terrestrial driving forces, respectively. IUR_{0G} and IUR_{1G}
 533 are the impurity uptake ratio for those forces, respectively. $C(\infty)$, $C(R)$, and Ce are protein
 534 concentrations away from the crystal, at the crystal surface and the saturated solution, respectively.
 535 $Ci(\infty)$ and $Ci(R)$ are the impurity concentration away from the crystal and the impurity concentration
 536 on the crystal's surface. β and βi are, respectively, the kinetic constants for the crystal growth of
 537 protein molecules and impurity molecules. D and Di are, respectively, the diffusion constants of
 538 protein molecules and impurity molecules. R is the crystal radius. IUR stands for the impurity uptake
 539 ratio.

540 It can be seen that when equations (1) and (2) are plotted on the abscissa with an $R\beta / D$ value,
 541 the effect of the formation of the concentration depletion zone increases as the $R\beta / D$ value increases.
 542 For details, see Ref. 52. A positive effect can be expected as R increases, as β increases, or as D
 543 decreases. Therefore, when diffusion is slow in the solution, while the crystal growth is fast, and the
 544 crystal grows large, greater effects can be expected for the space experiment.

545 The authors devised an approximate expression [33], which roughly estimates D , as well as an
 546 experimental method that roughly estimates β [53, 54]. That is, by observing the crystal growth time
 547 course in the batch method, we can estimate D and β . In evaluating the results of the space
 548 experiments of JAXA using this index, when D/β was 3 mm or less, there were effects of microgravity
 549 in about 70% of the crystals, such as the improvement of clustering and the improvement of X-ray
 550 diffraction resolution [55].

551 Based on the average value of the sizes of the generated crystals and the values of D and β , the
 552 $R\beta/D$ is calculated to be 0.035 or more. From this, the effect of IDZ (suppression of impurity uptake)
 553 is considered to be dominant in crystals with sizes used for X-ray diffraction experiments. On the
 554 other hand, when R is large (about 1 mm or more), like in the crystals used for the neutron diffraction
 555 experiments, both PDZ and IDZ effects can be expected.

556 *5.3. Measures to enhance the effects of space experiments*

557 From this estimation of the concentration depletion zone around the crystal, in order to
 558 positively enhance the effect of the space experiment, D should be decreased, and β should be
 559 increased. Since D depends on the viscosity of the solution, it is possible to use a highly viscous
 560 reagent, such as PEG. Optimizing the salt concentration in the solution is very important when
 561 crystallization conditions including PEG are applied to various kinds of protein samples [9]. On the

562 other hand, β is increased by refining the protein sample and increasing uniformity. For example, if
563 the lysozyme is purified by ion exchange chromatography to increase its homogeneity, β becomes
564 several times larger [54]. From these results, it is possible to determine in advance whether or not the
565 effects of the space experiment can be expected by determining the values of D and β beforehand. It
566 is also possible to improve the usefulness of the space experiments by improving the samples and
567 crystallization conditions that are inappropriate for space experiments with these promotional
568 measures [56, 57].

569 *5.4. Analysis of the transient crystal growth process*

570 The solution concentration around the crystal in actual protein crystallization is a transient
571 process that decreases as the crystal grows. That is, when nuclei are formed and crystal growth starts,
572 the degree of surface supersaturation is high, but at the end of crystal growth, the protein
573 concentration in the solution drops to the concentration of solubility. As a result, crystals will grow
574 from the center to the surface all under different supersaturation degrees. In addition, the amount of
575 impurities taken in varies depending on the location in the crystal.

576 The authors devised a numerical calculation model to determine the crystal growth process
577 closer to actual crystallization [58]. For the sake of simplicity, partial differential equations describing
578 both the diffusion process in the virtual sphere and the crystal growth process in the center of the
579 sphere are described.

580 By applying various constants of the crystallization process of the lysozyme to this model, the
581 impurity concentration is low in the portion close to the center in the crystals grown in microgravity,
582 while in the peripheral portion, the impurity concentration is higher than that of the crystals grown
583 on the ground [58, 59]. In this simulation, β is set to a constant value, but, in reality, β increases as the
584 impurity concentration decreases, as described above. Based on the results of the in-situ observation
585 of the NanoStep project by Tsukamoto et al. [60], in a microgravity environment where IDZ is formed,
586 as the impurity concentration decreases, the crystal growth rate became faster than that in the
587 terrestrial environment, and β becomes large. Therefore, the effect of PDZ and IDZ seems to be further
588 enhanced in microgravity. From this result, it is suggested that differences exist in the quality of the
589 X-ray diffraction patterns of crystals due to differences in the positions of the crystals. Therefore, the
590 authors investigated the local diffraction of crystals by growing crystals from a lysozyme sample
591 containing some impurities and performing X-ray diffraction experiments on the crystals with a grid
592 scan [59]. Although a preliminary experimental result, it was observed from the crystals obtained in
593 the terrestrial experiment that the a and b axes of the crystal lattice becomes slightly larger outward
594 from the center of the crystal. On the other hand, this phenomenon was not observed in the crystals
595 obtained from the space experiment. Crystals grown on the ground seem to have a large amount of
596 impurities taken up around the center of the crystal, and these impurities have a larger influence on
597 the lattice of the crystal toward the outside of the crystal.

598 *5.5. Other phenomena*

599 Ng et al. reported on crystallization in a microgravity environment for 6 months using the CD
600 method, where 2 mm square crystals were grown in a capillary with inner diameters of 2 mm [37]. In
601 this experiment, Ostwald ripening (i.e., the larger the crystal, the lower the solubility) resulted in
602 crystals becoming dissolved and absorbed into large crystals. Therefore, it is necessary to investigate
603 the extent to which this phenomenon can be applied to the formation of large crystals for structural
604 analysis, as well as the optimum conditions.

605 **6. Conclusion**

606 This paper summarizes the evaluation of the quality of protein samples and crystallization
607 conditions and the handling of the obtained crystals based on decades of experience, especially for
608 proteins acquired from the JAXA PCG space experiments. These technologies still have room for

609 improvement, and progress is being made daily. We hope that these technologies will lead to the
610 realization of practical and useful crystallization experiments.

611 **Author Contributions:** Section 1, H.T.; section 2, H.T., M.K., N.F. and K.I.; section 3, Y.H., M.K., N.F. and K.I.;
612 section 4, M.K., N.F. and K.I.; section 5, H.T.; section 6, H.T.; supervision, S.T. and H.T.

613 **Funding:** This research received no external funding.

614 **Acknowledgments:** We thank all the academic and research institutional users of the JAXA PCG experiments
615 for contributing protein samples to the microgravity experiments. Especially, we thank Professor Atsushi
616 Nakagawa of Osaka University for the H-protein sample, Professor Kiyohiko Igarashi of the University of Tokyo
617 for the Pccel6A sample, and Professor Tetsuya Masuda of Kyoto University for the thaumatin sample. We are
618 grateful to the European Space Agency and to Professor Garcia-Ruiz of CSIC-University of Granada for counter-
619 diffusion techniques and space crystallization technology. Finally, we are grateful to the members of the JAXA
620 PCG team.

621 **Conflicts of Interest:** The authors declare no conflict of interest.

1. Chernov, A.A. Protein crystals and their growth. *J. Struct. Biol.* **2003**, *142*, 3–21.
2. McPherson, A.; Gavira, J.A. Introduction to protein crystallization. *Acta Cryst.* **2014**, *F70*, 2–20.
3. Giege, R. A historical perspective on protein crystallization from 1840 to the present day. *FEBS Journal* **2013**, *280*, 6456–6497.
4. Candoni, N.; Grossier, R.; Hammadi, Z.; Morin, R.; Veesler, S. Practical Physics Behind Growing Crystals of Biological Macromolecules. *Protein & Peptide Letters*, **2012**, *19*(7), 714–724.
5. Matsuura, Y.; Chernov, A.A. Morphology and the strength of intermolecular contacts in protein crystals. *Acta Cryst.* **2003**, *D59*, 1347–1356.
6. Thomas, B.R.; Carter, D.; Rosenberger, F. Effect of microheterogeneity on horse spleen apoferritin crystallization. *J. Cryst. Growth* **1998**, *187*, 499–510.
7. Thomas, B.R.; Chernov, A.A. Acetylated lysozyme as impurity in lysozyme crystals: constant distribution coefficient. *J. Cryst. Growth* **2001**, *232*, 237–243.
8. Vekilov, P.G. Elementary processes of protein crystal growth. *Prog. Crystal Growth Charact.* **1993**, *26*, 25–49.
9. Yamanaka, M.; Inaka, K.; Furubayashi, N.; Matsushima, M.; Takahashi, S.; Tanaka, H.; Sano, S.; Sato, M.; Kobayashi, T.; Tanaka, T. Optimization of salt concentration in PEG-based crystallization solutions. *J. Synchrotron Rad.* **2010**, *18*, 84–87.
10. ExPASy Bioinformatics Resource Portal. <https://www.expasy.org/> (accessed May 8, 2019).
11. Garfin, D.E. One-dimensional gel electrophoresis. *Methods Enzymol.* **2009**, *463*, 497–513.
12. Van Der Laan, J.M.; Swarte, M.B.A.; Groendijk, H.; Hol, W.G.J.; Drenth, J. The influence of purification and protein heterogeneity on the crystallization of *p*-hydroxybenzoate hydroxylase. *Eur. J. Biochem.* **1989**, *179*, 715–724.
13. O'Farrell, P. High resolution two-dimensional electrophoresis of proteins. *J. Biol. Chem.* **1975**, *250*(10), 4007–4021.
14. Jungbauer, A.; Hahn, R. Ion-exchange chromatography. *Methods Enzymol.* **2009**, *463*, 349–371.
15. Cummins, P.M.; Rochfort, K.D.; O'Connor, B.F. Ion-exchange chromatography: Basic principles and application. In *Protein Chromatography. Methods in Molecular Biology*; ; Walls, D. Loughran, S., Eds.; Human Press, New York, USA, **2017**; 1485.
16. Proteau, A.; Shi, R.; Cygler, M. Application of dynamic light scattering in protein crystallization. *Curr. Protoc. Protein Sci.* **2010**, *61*, 17.10.1–17.10.9.
17. Tyler-Cross, R. & Schirch, V. Effects of amino acid sequence, buffers, and ionic strength on the rate and mechanism of deamidation of asparagine residues in small peptides. *J. Biol. Chem.*, **1991**, *266*, 22549–22556.
18. Majeed, S.; Ofek, G.; Belachew, A.; Huang, C.; Zhou, T.; Kwong, P. D. Enhancing protein crystallization through precipitant synergy. *Structure*, **2003**, *11*, 1061–1070.
19. Collins, K.D. Ions from the Hofmeister series and osmolytes: effects on proteins in solution and in the crystallization process. *Methods* **2004**, *34*, 300–311.
20. Tanaka, S.; Ataka, M. Protein crystallization induced by polyethylene glycol: A model study using apoferritin. *J. Chem. Phys.* **2002**, *117*(7), 3504–3510.
21. Newstead, S.; Ferrandon, S.; Iwata, S. Rationalizing alpha-helical membrane protein crystallization. *Protein Sci.* **2008**, *17*(3), 466–472.

662 22. Stetsenko, A.; Guskov, A. An Overview of the Top Ten Detergents Used for Membrane Protein
663 Crystallization. *Crystals* **2017**, *7*, 197.

664 23. García-Ruiz, J.M. Nucleation of protein crystals. *J. Struct. Biol.* **2003**, *142*, 22–31.

665 24. Yoshizaki, I.; Nakamura, H.; Fukuyama, S.; Komatsu, H.; Yoda, S. Estimation of crystallization boundary
666 of a model protein as a function of solute concentration and experiment time. *Int. J. Microgravity Sci. Appl.*
667 **2002**, *19*(1), 30–33.

668 25. Takahashi, S.; Yan, B.; Furubayashi, N.; Inaka, K.; Tanaka, H. Effects of polyethylene glycol 4000 and
669 Sodium Chloride: 3-dimensional phase diagram for a protein crystallization. *Materials Structure* **2016**, *23*(2),
670 154.

671 26. Jakoby, W.B. A technique for the crystallization of proteins. *Anal. Biochem.* **1968**, *26*, 295–298.

672 27. Nakamura, H.; Fukuyama, S.; Yoshizaki, I.; Yoda, S.-I. Theory of vapor diffusion in the high-density protein
673 crystal growth device and its application to the measurement of the vapor pressures of aqueous solutions.
674 *J. Cryst. Growth* **2003**, *259*, 149–159.

675 28. Benvenuti, M.; Mangani, S. Crystallization of soluble proteins in vapor diffusion for x-ray crystallography.
676 *Nat. Protoc.* **2007**, *2*(7), 1633–1651.

677 29. García-Ruiz, J.M.; González-Ramírez, L.A.; Gavira, J.A.; Otálora, F. Granada Crystallization Box: a new
678 device for protein crystallization by counter-diffusion techniques. *Acta Cryst.* **2002**, *D58*, 1638–1642.

679 30. Otálora, F.; Gavira, J.A.; Ng, J.D.; García-Ruiz, J.M. Counterdiffusion methods applied to protein
680 crystallization. *Prog. Biophys. Mol. Biol.* **2009**, *101*, 26–37.

681 31. García-Ruiz, J.M. Counterdiffusion method for macromolecular crystallization. *Methods Enzymol.* **2003**, *368*,
682 130–154.

683 32. Tanaka, H.; Inaka, K.; Sugiyama, S.; Takahashi, S.; Sano, S.; Sato, M.; Yoshitomi, S. A simplified counter
684 diffusion method combined with a 1D simulation program for optimizing crystallization conditions. *J. Synchrotron Rad.* **2004**, *11*, 45–48.

685 33. Tanaka, H.; Yoshizaki, I.; Takahashi, S.; Yamanaka, M.; Fukuyama, S.; Sato, M.; Sano, S.; Motohara, M.;
686 Kobayashi, T.; Yoshitomi, S.; Tanaka, T. Diffusion coefficient of the protein in various crystallization
687 solutions: The Key to growing high-quality crystals in space. *Microgravity sci. technol.* **2006**, *XVIII-3/4*, 91–
688 94.

689 34. McPherson, A. Practical procedures for macromolecular crystallization. In *Crystallization of Biological
690 Macromolecules*; Bianco, C. Ed.; Cold Spring Harbor: New York, USA, **1999**.

691 35. Maeda, M.; Chatake, T.; Tanaka, I.; Ostermann, A.; Niimura, N. Crystallization of a large single crystal of
692 cubic insulin for neutron protein crystallography. *J. Synchrotron Rad.* **2004**, *11*, 41–44.

693 36. Takahashi, S.; Koga, M.; Yan, B.; Furubayashi, N.; Kamo, M.; Inaka, K.; Tanaka, H. JCB-SGT crystallization
694 devices applicable to PCG experiments and their crystallization conditions. *Int. J. Microgravity Sci. Appl.*
695 **2019**, *36*(1), 360107.

696 37. Ng, J.D.; Baird, J.K.; Coates, L.; García-Ruiz, J.M.; Hodge, T.A.; Huang, S. Large-volume protein crystal
697 growth for neutron macromolecular crystallography. *Acta Cryst.* **2015**, *F71*, 358–370.

698 38. Nakamura, A.; Ishida, T.; Fushinobu, S.; Kusaka, K.; Tanaka, I.; Inaka, K.; Higuchi, Y.; Masaki, M.; Ohta, K.;
699 Kaneko, S.; Niimura, N.; Igarashi, K.; Samejima, M. Phase-diagram-guided method for growth of a large
700 crystal of glycoside hydrolase family 45 inverting cellulose suitable for neutron structural analysis. *J. Synchrotron Rad.* **2013**, *20*, 859–863.

701 39. “Crystal growth apparatus for biological macromolecules” Japan patent JP4161101B.

702 40. Takahashi, S.; Tanaka, H. Background of protein crystallization technologies in space. *Int. J. Microgravity
703 Sci. Appl.* **2017**, *34*(1), 340103.

704 41. Garman, E.F.; Schneider, T.R. Macromolecular Cryocrystallography. *J. Appl. Cryst.* **1997**, *30*, 211–237.

705 42. Day, J.; McPherson, A. Macromolecular crystal growth experiments on International Microgravity
706 Laboratory-1. *Protein Sci.* **1992**, *1*(10), 1254–1268.

707 43. Ng, J.D.; Sauter, C.; Lorber, B.; Kirkland, N.; Arnez, J.; Giege, R. Comparative analysis of space-grown and
708 earth-grown crystals of an aminoacyl-tRNA synthetase: space-grown crystals are more useful for structural
709 determination. *Acta Cryst.* **2002**, *D58*, 645–652.

710 44. McPherson, A.; DeLucas, L.J. Microgravity protein crystallization. *npj Microgravity* **2015**, *1*, 15010.

711 45. Snell, E.H.; Helliwell, J.R. Macromolecular crystallization in microgravity. *Rep. Prog. Phys.* **2005**, *68*, 799–853.

712 46. Maes et al., Toward a Definition of X-ray Crystal Quality. *Cryst. Growth Des.*, **2008**, *8* (12), 4284–4290

715 47. Otálora, F.; Novella, M.L.; Gavira, J.A.; Thomas, B.R.; García-Ruiz, J.M. Experimental evidence for the
716 stability of the depletion zone around a growing protein crystal under microgravity. *Acta Cryst.* **2001**, D57,
717 412–417.

718 48. Thomas, B.R.; Chernov, A.A.; Vekilov, P.G.; Carter, D.C. Distribution coefficients of protein impurities in
719 ferritin and lysozyme crystals Self-Purification in microgravity. *J. Cryst. Growth*, **2000**, 211, 149–156.

720 49. Vekilov, P.G.; Thomas, B.R.; Rosenberger, F. Effects of convective solute and impurity transport in protein
721 crystal growth. *J. Phys. Chem. B*, **1998**, 102, 5208–5216.

722 50. Adachi, H.; Takano, K.; Matsumura, H.; Inoue, T.; Mori, Y.; Sasaki, T. Protein crystal growth with a two-
723 liquid system and stirring solution. *J. Synchrotron Rad.*, **2004**, 11(1), 121–124.

724 51. Chernov, A.A. Crystal growth and crystallography. *Acta Cryst.* **1998**, A54, 859–872.

725 52. Inaka, K.; Tanaka, H.; Takahashi, S.; Sano, S.; Sato, M.; Shirakawa, M.; Yoshimura, Y. Numerical Analysis
726 of the diffusive field around a growing protein crystal in microgravity. *Defect and Diffusion Forum*. **2012**,
727 323–325, 565–569.

728 53. Tanaka, H.; Inaka, K.; Sugiyama, S.; Takahashi, S.; Sano, S.; Sato, M.; Yoshitomi, S. Numerical Analysis of
729 the depletion zone formation around a growing protein crystal. *Ann. N.Y. Acad. Sci.* **2004**, 1027, 10–19.

730 54. Tanaka, H.; Inaka, K.; Furubayashi, N.; Yamanaka, M.; Takahashi, S.; Sano, S.; Sato, M.; Shirakawa, M.;
731 Yoshimura, Y. Controlling the diffusive field to grow a higher quality protein crystal in microgravity.
Defect and Diffusion Forum. **2012**, 323–325, 549–554.

733 55. Takahashi, S.; Ohta, K.; Furubayashi, N.; Yan, B.; Koga, M.; Wada, Y.; Yamada, M.; Inaka, K.; Tanaka, H.;
734 Miyoshi, H.; Kobayashi, T.; Kamigaichi, S. JAXA protein crystallization in space: ongoing improvements
735 for growing high-quality crystals. *J. Synchrotron Rad.* **2013**, 20, 968–973.

736 56. Tanaka, H.; Tsurumura, T.; Aritake, K.; Furubayashi, N.; Takahashi, S.; Yamanaka, M.; Hirota, E.; Sano, S.;
737 Sato, M.; Kobayashi, T.; Tanaka, T.; Inaka, K.; Urade, Y. Improvement in the quality of hematopoietic
738 prostaglandin D synthase crystals in a microgravity environment. *J. Synchrotron Rad.* **2011**, 18, 88–91.

739 57. Inaka, K.; Takahashi, S.; Aritake, K.; Tsurumura, T.; Furubayashi, N.; Yan, B.; Hirota, E.; Sano, S.; Sato, M.;
740 Kobayashi, T.; Yoshimura, Y.; Tanaka, H.; Urade, Y. High-quality protein crystal growth of mouse
741 lipocalin-type prostaglandin D Synthase in microgravity. *Cryst. Growth Des.* **2011**, 11, 2107–2111.

742 58. Tanaka, H.; Sasaki, S.; Takahashi, S.; Inaka, K.; Wada, Y.; Yamada, M.; Ohta, K.; Miyoshi, H.; Kobayashi, T.;
743 Kamigaichi, S. Numerical model of protein crystal growth in a diffusive field such as the microgravity
744 environment. *J. Synchrotron Rad.* **2013**, 20, 1003–1009.

745 59. Takahashi, S.; Nakagawa, A.; Furubayashi, N.; Inaka, K.; Ohta, K.; Tanaka, H. Non-uniform diffractive
746 quality of the crystals grown in microgravity and in terrestrial gravity. *J. Jpn Association for Crystal Growth*
747 **2016**, 43(2), 110–116.

748 60. Tsukamoto, K. Growth rate of protein crystals under microgravity. *J. Jpn. Soc. Microgravity Appl.* **2012**, 29(3),
749 106–110.

750